arXiv:1409.6418v3 [astro-ph.SR] 23 Oct 2014

Coronal Heating Driven by A Magnetic Gradient Pumping Mechanism in Solar Plasmas

Baolin Tan
Key Laboratory of Solar Activity, National Astronomical Observatories of Chinese Academy of Sciences, Datun Road 20A, Chaoyang District, Beijing 100012, China; bltan@nao.cas.cn

ABSTRACT

The heating of the solar coronal is a longstanding mystery in astrophysics. Considering that the solar magnetic field is spatially inhomogeneous with a considerable magnetic gradient from the solar surface to the corona, this work proposes a magnetic gradient pumping (MGP) mechanism to try to explain the formation of hot plasma upflows, such as hot type II spicules and hot plasma ejections. In the MGP mechanism, the magnetic gradient may drive the energetic particles to move upward from the underlying solar atmosphere and form hot upflows. These upflow energetic particles are deposited in the corona, causing it to become very hot. Rough estimations indicate that the solar corona can be heated to above 1 million degrees, and the upflow velocity is about 40 km s^{-1} in the chromosphere and about 130 km s^{-1} in the corona. The solar magnetic flux tubes act as pumpers to extract energetic particles from the underlying thermal photosphere, convey them, and deposit them in the corona. The deposit of these energetic particles causes the corona to become hot, and the escape of such particles from the photosphere leaves it a bit cold. This mechanism can present a natural explanation to the mystery of solar coronal heating.

Subject headings: plasmas – stars: coronae – Sun: atmosphere – Sun: corona

Online-only material: color figures

1. Introduction

As early as the 1940's, it was known that the solar corona is hot enough that the temperature can exceed one million degrees, which is about two orders of magnitude hotter than the temperature in the underlying photosphere (Edlen 1943). It is believed that the energy heating the corona comes from the solar interior. We also believe that the solar magnetic field must play a key role in heating and sustaining the hot corona. As for the heating power requirement (P_H), Aschwanden et al. (2007) estimate about $2\times10^5 \leq P_H \leq 2\times10^6$ erg $cm^{-2}s^{-1}$ in active regions, about $1\times10^4 \leq P_H \leq 2\times10^5$ erg $cm^{-2}s^{-1}$ in quiet-Sun regions, and about $5\times10^3 \leq P_H \leq 1\times10^4$ erg $cm^{-2}s^{-1}$ in coronal holes. There is still debate over how the magnetic field transports the energy from the solar interior to the outer atmosphere and how the energy is deposited once it reaches the corona. According to thermodynamic laws, if only the thermal conduction mechanism is at work, the temperature must steadily drop from the photosphere to the corona with increasing height. The heating mechanism of the extreme hot corona has puzzled astrophysicists and theoreticians for more than 70 years. To solve this big mystery, we must answer three key problems. (1) What is the energy source? (2) How is the energy transported from the source region into the corona? (3) How does the energy dissipate into heat?

A number of models have been proposed to solve this mystery. Comprehensive reviews of this issue can be found in Narain & Ulmschneider (1996), Walsh & Ireland (2003), and Klimchuk (2006) among others. These models can be classified into two types. (1) Wave mechanisms in which the solar violent inner motions of the Sun cause the magnetic field lines to oscillate, transporting energy through the cold underlying atmosphere and depositing it into the corona via

magnetohydrodynamic wave dissipations (Davila 1987). The type of wave most frequently mentioned in these models is Alfven wave (Heyvaerts & Priest 1983; Davila 1987; Wu & Fang 2003; De Pontieu et al. 2007; Jess et al. 2009; van Ballegooijen et al. 2011; Chen & Wu 2012; etc.). The key problem with such models is how these waves dissipate their energy and heat the plasma in the corona, although many works show that the waves can carry enough energy to sustain the hot coronal temperatures (De Pontieu et al. 2007; Kerr 2012). (2) Reconnection mechanism in which the violent inner motions of the Sun cause the magnetic field lines to twist and trigger multiple magnetic reconnections with various scales in the upper atmosphere, releasing energy in the form of nanoflares that will heat and accelerate the coronal plasmas (Parker 1988; Sturrock 1999; Cargill & Klimchuk 2004; Rappazzo et al. 2008; etc.). However, the most unresolved problem with magnetic reconnection mechanism models is whether nanoflares can carry enough energy to heat the solar corona.

Recently, researchers conducting a series of observational discoveries have proposed explanations for coronal heating including hot plasma ejections along the ultrafine magnetic loop channels from the solar surface upward to the corona (Ji et al. 2012), hot upflows of type II spicules (De Pontieu et al. 2009, 2011), and rotating magnetic networks such as magnetic tornadoes (Wedemeter-Böhm et al. 2012) and EUV cyclones (Zhang & Liu 2011). In particular, ubiquitous type II spicules, which are hot upflows in fountain-like plasma jets that have been observed at extreme ultraviolet (EUV) wavelengths by the Atmospheric Imaging Assembly (AIA) on board NASA's *Solar Dynamics Observatory* (*SDO*), can heat the plasma to hundreds of thousands of degrees on their way to the corona, with a small fraction reaching a million degrees. This can be considered a possible candidate for explaining the coronal heating (De Pontieu et al. 2011). However, there is no theory yet to explain how the hot upflows form or why they become heated.

In this work, we propose that the ubiquitous magnetic gradient in the solar atmosphere may provide a pumping mechanism that picks up the fast and relatively high energy charged particles from the underlying thermal plasmas, drives them to move upward, and deposits them in corona, increasing the average kinetic energy and causing the corona to become very hot. This new model is called the magnetic gradient pumping (MGP) mechanism and may explain the several recent discoveries noted above. In Section 2 we discuss the magnetic configuration in the solar atmosphere, from the solar photosphere to the corona. Section 3 presents the deduction of the MGP mechanism in different magnetic configurations and their explanation of the above recent discoveries. Finally, the conclusion and some discussions are presented in Section 4.

2. Magnetic Configuration in Solar Atmosphere

It is well known that the solar magnetic field is highly inhomogeneous and this inhomogeneity plays a dominant role in almost all processes in the solar atmosphere. Since magnetic fields are frozen in the coronal plasmas, soft X-ray or EUV imaging observations may present the configuration of the coronal magnetic field. Such observations show that the fundamental structure of the solar magnetic field is magnetic flux tubes (Zwaan 1978), which can be sorted into two types (Fisk & Schwadron 2001; Aschwanden & Nightingale 2005; Litwin & Rosner 1993): open magnetic flux tubes and closed magnetic flux loops.

1. In open magnetic flux tubes, the magnetic field lines remain attached to the solar photosphere and are dragged outward into the higher corona or even stretched into the remote heliosphere (Fisk & Schwadron 2001). They may be associated with solar streamers, solar winds, solar radio type III bursts (Reid & Ratcliffe 2014), etc.

2. In closed magnetic flux loops, the field lines remain connected with opposite magnetic polarities entirely attached to the photosphere and form multi-scale loops and active regions. They are possibly related to various solar eruptions (López Fuentes et al. 2006).

Practically, since the EUV line 171 Å forms from Fe IX, its formation temperature is about 6.3×10^5 K, very closed to the interface between the transition region and corona (Lemen et al. 2012). So, when a magnetic flux tube in the AIA 171 Å image extends deeply into the corona without a visible looptop, it can be regarded as an open flux tube, while a magnetic flux tube connects one

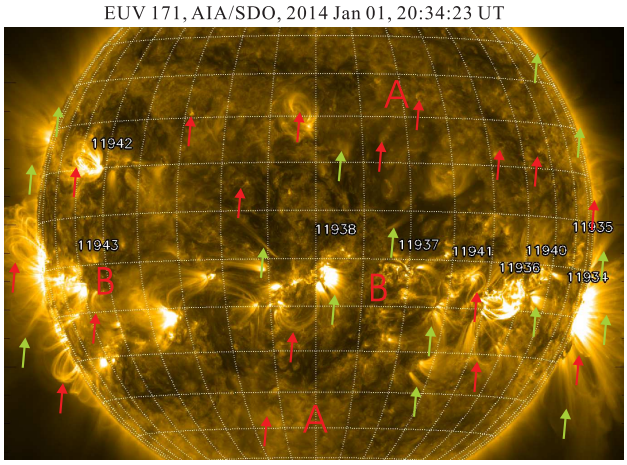

Fig. 1.— EUV imaging observation of the solar disk at 171 Å at 20:34:23 UT on 2014 January 1 obtained by AIA/SDO. Here, the open magnetic flux tubes (green arrows) and the closed magnetic flux loops (red arrows) can be found to have different spatial scales in the quiet region (A) and active regions (B).

footpoint to another via a visible looptop in the AIA 171 Å image it can be regarded as a closed magnetic flux loop. Of course, this classification is made relatively. Figure 1 presents a recent imaging observation at 171 Å observed by AIA/SDO with a pixel size of $0''.6$ on 2014 January 1. It is obvious that either in the solar quiet regions (marked as A) or in the active regions (marked as B), the magnetic configuration is composed of open magnetic flux tubes (such as the place marked by green arrows) and closed magnetic flux loops (such as the place marked by red arrows). Actually, when we investigate a large closed magnetic flux loop, such as big loops across different active regions, the local part around one footpoint can be approximately regarded as an open magnetic flux tube.

The common property of both types of configurations is that they have a divergent structure with a considerable magnetic gradient from the footpoints to the higher place. In fact, from imaging observations, when we track a single coronal loop from one footpoint via looptop to another footpoint, the loop's cross section is approximately constant, but when we investigate a bundle of coronal loops, we may find that they are diverging from their footpoints to the higher corona. In such configurations, the magnetic gradients are ubiquitous. Many researchers have tried to obtain the magnetic gradients in solar atmosphere (Hagyard et al. 1983; Landolfi 1987; Liu et al. 1996; Mathew & Ambastha 2000; etc.). Gelfreikh et al. (1997) obtained a coronal magnetic gradient of 10^{-4} G km^{-1} at a height of 10^5 km with a magnetic field strength of about 20 G. However, so far, it is still very difficult to obtain the magnetic gradients in the solar atmosphere from observations.

3. Magnetic Gradient Pumping Mechanism

Schluter (1957) proposed that non-magnetized material bulk can be pushed to move rapidly in an external diverging magnetic field as a diamagnetic body and the acceleration is proportional to

$$-\nabla(logB^2) \tag{1}$$

Here B is the external magnetic field. This idea is called the melon-seed mechanism (Pneuman 1984). Many people adopted this mechanism to explain the formation of solar surges, spicules, jets, filaments, coronal mass ejections (CMEs), and solar wind expansion (Altschuler et al. 1968; Pneuman 1983; Hollweg 2006; Filippov et al. 2007, 2009; Parashar et al. 2013). This mechanism can explain the motion of the bulk of diamagnetic plasmas, but it cannot explain why the corona is much hotter than the underlying chromosphere and photosphere. Here, we investigate the kinetic behaviors of single charged particles in open and closed solar magnetic flux tubes. We find that different particles with different kinetic energies have different motions.

3.1. In Open Magnetic Flux Tubes

Consider a charged particle moving in an open magnetic flux tube with a converging region near the photosphere and a diverging region in the corona and with a transverse velocity $v_t \neq 0$; it will gyrate around the magnetic field lines in a circular or helical orbit. The coupling of the radial component of the magnetic field and the particle's transverse motion will produce an equivalent driving force parallel to the magnetic field lines and

pointing to a weak magnetic field region (Figure 2). This force is called the magnetic gradient force (F_m):

$$F_m = -\mu \nabla B = -G_B \epsilon_t \tag{2}$$

Here, $\mu = \frac{\epsilon_t}{B}$ is the particle's magnetic moment which is approximately an invariance $\epsilon_k = \epsilon_t + \epsilon_l$ where $\epsilon_t = \frac{1}{2} m v_t^2$ is the transverse kinetic energy, $\epsilon_l = \frac{1}{2} m v_l^2$ is the longitudinal kinetic energy, m is the particle's mass, and v_t and v_l are the transverse and longitudinal velocities, respectively. $G_B = \frac{\nabla B}{B}$ is the relative magnetic gradient. The absolute value of its reciprocal is the magnetic field scale height $L_B = \frac{1}{|G_B|} = |\frac{B}{\nabla B}|$.

Equation (2) is very similar to Equation (1). However, they are intrinsically different. Equation (1) only presents the magnetic tension force acting on the bulk of diamagnetic materials in a diverging field, while Equation (2) expresses the driving force acting on a particle in a diverging magnetic field.

Here, there is another problem: Equation (2) works only in collisionless plasmas where magnetic moment is conserved. The photosphere, however, is highly collisional. As we know, the collision frequency is proportional to the plasma density n_p, and is inversely proportional to $T^{3/2}$. T is the temperature. Similar to the magnetic gradient, there is also a dominating density gradient from the solar photosphere to the upper atmosphere (chromosphere and corona), and the collision probability of a particle will decrease rapidly from the underlying strong magnetic field region to the upper weak field region. When a charged particle moves from the dense photosphere to the tenuous corona, it is reasonable to assume that the particle's magnetic moment is still approximately conserved. Equation (2) is still approximately valid in this regime.

In fact, L_B changes with height (h) in the solar atmosphere. It approximates to $\sim$ 1000 km near the photosphere, $\sim$ 2000 km in the chromosphere, and larger than 2×10^4 km in the low corona (Gelfreikh et al. 1997; Verth et al. 2011). The magnetic gradient in the solar open magnetic flux tube is downward, therefore F_m directs upward. The higher the transverse kinetic energy (ϵ_t), the faster the particle moves upward. This leads to separation of high-energy particles from lower energy particles. When energetic particles are transported to the higher place and reach a new thermal equilibrium through thermal collisions, they reach a high temperature. As high-energy particles escape, the average kinetic energy of the underlying adjacent plasma (e.g., around footpoints) will decrease and cool down slightly.

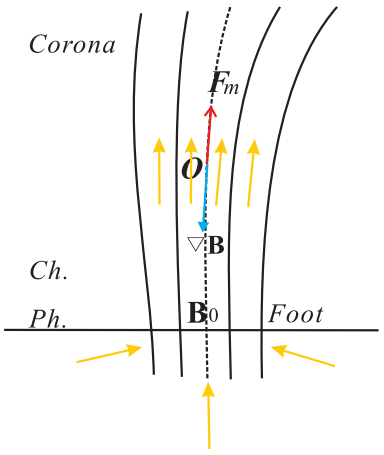

Fig. 2.— Schematic diagram of an open magnetic flux tube. A charged energetic particle at photosphere (Ph) will be driven to move upward via the chromosphere (Ch) and into corona. B_0 is the magnetic field at the footpoints and d is the distance between footpoints. The blue and red arrows indicate the magnetic gradient and its driving force (F_m), respectively. Yellow arrows show propagations of energetic particles.

In real magnetic flux tubes, besides the magnetic gradient force F_m, the charged particles are also affected by the solar gravitational force $F_g = mg(h)$. The net upward force acting on particles can be expressed as

$$f_t \simeq -G_B \epsilon_t - mg(h). \tag{3}$$

Here, $g(h)$ is the solar gravitational acceleration at height h, $g(0) \simeq 274$ m s^{-2} near the photosphere. Only when $f_t > 0$ can the energetic particles be driven upward. Therefore, a starting energy (ϵ_{t0}) for the upward motion can be deduced:

$$\epsilon_{t0} = mg(h) L_B. \tag{4}$$

Here we find that the starting energy is proportional to the mass of the particle. Heavy ions have

a higher starting energy and this leads to a consequence that only the very high energy heavy particles can be driven to move upward to the higher corona. For example, Oxygen ions or metal ions will have several times or decades of a proton's starting energy. In an open magnetic configuration, the charged particles can be divided into two groups:

1. Confined particles, $\epsilon_t < \epsilon_{t0}$, which are confined in the lower region of the magnetic configuration by the solar gravitational force. Obviously, confined particles are distributed in the lower energy part of the thermal distribution profile.

2. Escaping particles, $\epsilon_t > \epsilon_{t0}$, which can be driven to move upward along the magnetic flux tube. They are distributed in the high-energy tail of the thermal distribution function. Supposing that the solar photospheric plasma has a Maxwellian distribution at temperature T_0, the plasma density is N_0. The number of escaping particles can be calculated as

$$N(\epsilon_t > \epsilon_{t0}) = qN_0 \int_{\epsilon_{t0}}^{\infty} f(\epsilon_k) d\epsilon_k \tag{5}$$

Here, $f(\epsilon_k) = 2\pi[\frac{\epsilon_k}{(\pi k_B T_0)^3}]^{\frac{1}{2}} e^{-\frac{\epsilon_k}{k_B T_0}}$, k_B is the Boltzman constant. q is a factor indicating the fraction of ϵ_t in total kinetic energy, $q \sim 0.5$ for simplicity. The total energy carried by escaping particles is

$$E(\epsilon_t > \epsilon_{t0}) = qN_0 \int_{\epsilon_{t0}}^{\infty} f(\epsilon_k) \epsilon_k d\epsilon_k \tag{6}$$

The energetic particles escape from the underlying atmosphere, reach a higher place, and reach thermal equilibrium by continuous collisions. The particle's average kinetic energy can be regarded as an estimation of the temperature:

$$T_c = \frac{E(\epsilon_t > \epsilon_{t0})}{k_B N(\epsilon_t > \epsilon_{t0})} \tag{7}$$

Assuming $L_B = 1000$ km near the photosphere, the starting energy ϵ_{t0} is 0.0016 eV for electrons and 2.85 eV for protons. Here, the starting energy of electrons is much smaller than that of ions. It seems that a great majority of electrons and only a small part of ions can be driven to move upward. In fact, as the electrostatic attraction between electrons and ions will hold back electrons and drag ions upward to avoid the spatially charged separation, ions will play a key role in the above regime. It is reasonable to adopt the starting energy of ions as the lower limit in the above integrating calculations. When $\epsilon_k > \epsilon_{t0}$ and the charged particle moves from the lower strong field region (e.g. near the photosphere) upward to the upper weak field region (e.g., the corona), its transverse kinetic energy will convert gradually into longitudinal kinetic energy. When ϵ_t gets smaller and smaller and finally diminishes, the particle approaches to a maximum longitudinal velocity. The higher the initial total kinetic energy, the faster the particle moves upward. The higher energy particles more easily reach a higher region with fast longitudinal velocity and form a steady hot upflow. The velocity of upflows can be estimated as

$$v_{up} = \frac{\int_{\epsilon_{t0}}^{\infty} f(\epsilon_k) \sqrt{\frac{2\epsilon_k}{m}} d\epsilon_k}{\int_{\epsilon_{t0}}^{\infty} f(\epsilon_k) d\epsilon_k}. \tag{8}$$

The energy flow can be roughly estimated by

$$P_{up} \simeq k_B T_c \cdot N(\epsilon \geq \epsilon_{t0}) \cdot v_{up} \tag{9}$$

When the underlying atmosphere loses energy $E(\epsilon_t > \epsilon_{t0})$ to the upflow of escaping particles, it drops to a low temperature:

$$T_s = \frac{N_0 k_B T_0 - E(\epsilon_t > \epsilon_{t0})}{k_B [N_0 - N(\epsilon_t > \epsilon_{t0})]} \tag{10}$$

The deficit of energetic particles in the thermal atmosphere can be compensated for by the ambient and solar interior plasmas through thermal diffusions and interior convection. The yellow arrows in Figure 2 indicate the propagating direction of the energetic particles from the solar interior to the corona.

Generally, near the solar photosphere, $N_0 \simeq 10^{14}$ cm^{-3}, $T_0 \simeq 6000$ K (Vernazza et al. 1981). After the filtration of magnetic gradient force, we may obtain: $T_s \sim 5933$ K, $N(\epsilon_t > \epsilon_{t0}) \simeq 5.88 \times 10^{11}$ cm^{-3}, and $T_c \sim 3.94 \times 10^4$ K, $v_{up} \simeq 25.5$ km s^{-1}, and energy flow $P_{up} \simeq 8.19 \times 10^6$ erg cm$^{-2}s^{-1}$. These values are very close to that in the solar chromosphere at about 2000 km height (Vernazza et al. 1981).

In the solar chromosphere, the magnetic gradient becomes increasingly weaker and L_B becomes increasingly longer than that near the photosphere. Simply, we suppose that $L_B \sim 2000$ km, and the temperature is about 3.94×10^4 K. Then we obtain $N(\epsilon_t > \epsilon_{t0}) \simeq 1.01 \times 10^{11}$ cm^{-3}, $T_c \sim 1.12 \times 10^5$ K, $v_{up} \simeq 42.4$ kms^{-1}, and the energy flow $P_{up} \simeq 6.66 \times 10^6$ erg cm$^{-2}s^{-1}$. These values are very close to that in the solar transition region between the chromosphere and the corona at about 2000-3000 km in height.

In the solar transition region, supposing: $L_B \sim 5000$ km, $T_0 \sim 1.12 \times 10^5$ K. Then $N(\epsilon_t > \epsilon_{t0}) \simeq 2.03 \times 10^{10}$ cm^{-3}, $T_c \sim 2.97 \times 10^5$ K, $v_{up} \simeq 68.9$ kms^{-1}, and energy flow $P_{up} \simeq 5.76 \times 10^6$ erg cm$^{-2}s^{-1}$. These parameters are very close to that in the upper part of the solar transition region or at the bottom part of the solar corona.

Furthermore, near the bottom of the solar corona: $L_B \sim 3.0 \times 10^4$ km, $T_0 \sim 2.97 \times 10^5$ K. Then $N(\epsilon_t > \epsilon_{t0}) \simeq 3.52 \times 10^8$ cm^{-3}, $T_c \sim 1.06 \times 10^6$ K, $v_{up} \simeq 132.9$ kms^{-1}, and energy flow $P_{up} \simeq 6.91 \times 10^5$ erg cm$^{-2}s^{-1}$. These values are similar to the condition in the solar corona.

The above estimations indicate that the solar chromosphere and corona can be heated by a cascading filtration driven by magnetic gradient force. The estimated values of the upflow velocities are very close to those of type II spicules observed by AIA/SDO and Hinode (De Pontieu et al. 2011) and can present a reasonable explanation of the formation of type II spicules and other hot plasma upflows. The open magnetic flux tube acts as a pumper to extract the energetic particles from the underlying thermal photosphere and transport them to and deposit them in the corona. This process can be called as the MGP mechanism.

Actually, the magnetic gradient force is an equivalent effect parallel and opposite to the magnetic gradient ∇B, which acts on the guiding center and filtrates charged particles by their kinetic energies. In these processes, the magnetic field can not do any extra work on the charged particles; the total energy must be conservative. When magnetic gradient force causes the longitudinal kinetic energy (ϵ_l) to increase, the transverse kinetic energy (ϵ_t) decreases simultaneously. The energy conversion takes place between ϵ_t and ϵ_l. When ϵ_t is converted fully into ϵ_l, the magnetic gradient force disappears and a stable upflow forms.

In fact, charged energetic particles will not move upward endlessly. Because the magnetic field becomes homogenous in the higher corona, the magnetic gradient gradually vanishes ($G_B \sim 0$) and the magnetic gradient force also fades away ($F_m \sim 0$). When the condition $G_B < \frac{mg(h)}{\epsilon_t}$ is fulfilled, the net upward force becomes negative, $f_t < 0$. The particles are decelerated by solar gravitational force.

With the MGP mechanism, the escaping particle's transverse kinetic energy will convert into longitudinal kinetic energy, which will result in a temperature anisotropy in the coronal plasmas; the ion's longitudinal temperature (T_l) will be higher than the transverse temperatures (T_t). This property may explain ion temperature anisotropy in the solar winds (Hahn & Savin 2013). The temperature anisotropy triggers a series of plasma instabilities and leads to secondary energy release and the formation of thermal isotropic distributions.

3.2. In Closed Magnetic Flux Loops

Closed magnetic flux loops with various length scales are ubiquitous in the solar chromosphere and corona. They connect one magnetic polarity to the other in sunspots in active regions as well as connecting one side to another in the magnetic network of granules in solar-quiet regions (Priest et al. 2002). They are always associated with many phenomena such as solar active regions and flares, CMEs, (Aschwanden & Nightingale 2005), and X-ray and EUV bright points in the quiet Sun (Golub et al. 1977; Habbal & Withbroe 1981). Besides being located in active regions, closed magnetic flux loops also exist in solar-quiet regions with relatively small scales (Centeno et al. 2007). This property can also be seen in Figure 1.

When a particle leaves one footpoint of the closed magnetic flux loop, as the relative longitudinal magnetic gradient is downward $G_B < 0$, the particle will be driven to move upward by an upward magnetic gradient force (Figure 3). Considering the solar gravitational force $mg(h)$, the net force acting on the particle can be expressed as

$$f_t = -G_B(h)\epsilon_t \sin\alpha - mg(h) \qquad (11)$$

Here, α is the angle between the magnetic field

line and the horizontal direction, which will be near zero around the looptop. Particles can be activated to move upward only when $f_t > 0$. Then a starting energy can be deduced:

$$\epsilon_{t0} = mg(h)L_B \sin^{-1}\alpha \qquad (12)$$

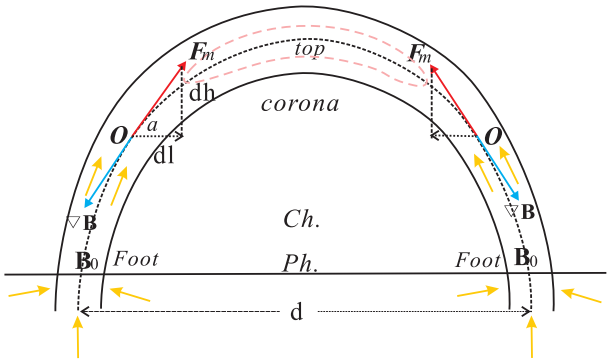

Fig. 3.— Schematic diagram of closed magnetic flux loops. B_0 is the magnetic field at the footpoints and d is the distance between footpoints. The blue and red arrows indicate the magnetic gradient and its driving force (F_m), respectively. Yellow arrows show the propagating flow of energetic particles. The dashed pink curve presents the trajectory of bounce particles.

Supposing the magnetic field is approximately one dipole in closed magnetic flux loops, it can be approximated as (Takakura & Scalise 1970): $B(h) = (\frac{1}{1+h/d})^3 B_0$. Here d is the distance between the two footpoints and h is the height. Then $\frac{\partial B}{B\partial l} = \frac{1}{B(h)}\frac{\partial B}{\partial h}\frac{\partial h}{\partial l} = -\frac{3}{d+h}\sin\alpha$, $L_B = (d + h)/3$. The magnetic gradient diminishes around the looptop gradually. The starting energy of the particles near the footpoint can be obtained as: $\epsilon_{t0} \simeq \frac{1}{3}mdg(0)$. According to the particle's kinetic energy (ϵ_k) and the initial incident angle (θ), all particles can be classified into three groups

1. *Confined particles.* When the kinetic energy $\epsilon_k < \epsilon_{t0}$, the particle is confined in the underlying photospheric atmosphere. Of course, the confined particles just have lower energy.

2. *Passing particles.* When the kinetic energy $\epsilon_k > \epsilon_{t0}$ and its initial incident angle (θ) is smaller than the magnetic mirror critical angle (θ_c), $\theta < \theta_c$, the particle can be driven to move upward from one footpoint, pass the looptop and precipitate at another footpoint. Here, the magnetic mirror critical angle $\theta_c = arcsin\sqrt{1/R_m}$. $R_m = B_{max}/B_{min}$ is the magnetic mirror ratio. B_{max} and B_{min} are the maximal and minimal magnetic field strength in the loop, respectively. Theoretically, the fraction of the passing particles is about $(2R_m)^{-1}$.

3. *Bounce particles.* When the kinetic energy $\epsilon_k > \epsilon_{t0}$ and its initial incident angle $\theta > \theta_c$, the particle will be driven to move upward from the footpoints, and bounce back and forth around the looptop (shown as the dashed pink curve in Figure 3). The number of energetic bounce particles can be estimated by

$$N_b = q_m q N_0 \int_{\epsilon_{t0}}^{\infty} f(\epsilon_k) d\epsilon_k \qquad (13)$$

Here, $q_m \simeq 1 - (2R_m)^{-1}$ indicates the fraction of bounce particles in the total particles.

When we investigate one-half of a closed magnetic flux loop, we find that the regime is very similar to that in an open magnetic flux tube. It is reasonable to assume that the energetic particles will be driven to move similar to what is shown in Figure 2. When energetic particles leave the footpoint, they will be driven to move upward. After this filtration (in fact, the filtration varies continuously from the footpoint to the looptop), the area around the looptop will be gathering energetic particles. When these energetic particles reach a new thermal equilibrium by collision or instability evolution, the temperature will become hotter than the underlying atmosphere. Supposing a semicircle magnetic flux loop $h = d/2$ and d=10^4 km, the magnetic field scale height near the footpoint is about 1000 km. Then $R_m = 3.75$, $q_m \simeq 0.87$, $\epsilon_{t0} \sim 9.5$ eV. The density of bounce particles is about $N_b \simeq 1.02 \times 10^{11}$ cm^{-3} with average thermal temperature of about 1.63×10^5 K. These values are very similar to the observations of the loop with length of about 5000 km. The dashed pink curve in Figure 3 shows the hot region in the closed magnetic flux loop. Around the looptop, the particle's longitudinal kinetic energy is much greater than its transverse kinetic energy, and the temperature is also anisotropic around the top region. As in the open magnetic flux tubes, the temperature anisotropy will trigger plasma insta-

bilities and lead to secondary energy release and finally form a thermal isotropic distribution (Dong et al. 1999).

In fact, there are various scales of closed magnetic flux loops in the solar atmosphere. They may connect one side of a network magnetic field to the other or connect an intranetwork magnetic field to a different network magnetic field, and could connect one polarity to another in sunspots, or even connect different active regions (Lin 1995; Lin & Rimmele 1999). The different scales of closed magnetic flux loops extend to different heights in the solar atmosphere. With the above MGP mechanism, the looptops will become very hot. Figure 4 presents the schematic diagram of the closed magnetic flux loop system with various scales. The thick parts with pink or red colors show the hot region around the looptops. The large amount of hot looptops may form the hot chromosphere and the much hotter corona.

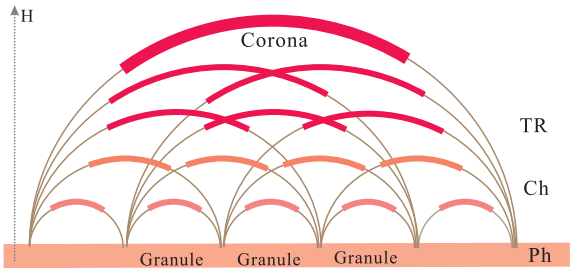

Fig. 4.— Schematic diagram of the magnetic flux loops from the photosphere (Ph) via the chromosphere (Ch) and the transition region (TR) to the corona. The thick parts with pink or red colors show the hot regions in the loops.

Additionally, when the energetic particles pile up and accumulate, the density will increase as well as the temperature around the looptops. Consequently, the plasma thermal pressure $p_t = nk_BT$ also increases. In an ideal situation, when the plasma pressure exceeds the magnetic pressure $p_m = \frac{B^2}{2\mu_0}$ ($\beta = \frac{p_t}{p_m} \geq 1$), the magnetic pressure cannot balance the expanding trend of the plasma thermal pressure. Then the magnetized plasma loop will break away from the confinement of the magnetic field, disrupting it, and lead to a violent energy release. From the balance between the plasma pressure and magnetic pressure ($p_t = p_m$), a density limit can be obtained:

$$n_m = \frac{B^2}{2\mu_0 k_B T} \tag{14}$$

For example, suppose that the looptop has a temperature of about 2 MK, and the magnetic field strength is about 50 Gs, then the density limit is about 3.5×10^{11} cm^{-3}.

In fact, tokamak plasma experiments indicate that the β limit is always smaller than the unit ($\beta_0 < 1$, it means $p_t < p_m$), and the density limit is also lower than that obtained from Equation (14). The real value depends on the boundary conditions (Haas & Thomas 1973; Greenwald et al. 1988; Greenwald 2002), such as the radii of the magnetic loop and its cross-section, the magnetic distribution in the section, etc. Generally, in recent tokamak experiments, $\beta_0 < 10\%$. Therefore, the limit density may be one order smaller than that deduced from Equation (14).

When the density of the hot plasma exceeds the limit, the energetic particles may get free from the confinement of the magnetic field and spread to the adjacent plasma. The final result leads to annihilation of the loop (Inverarity & Priest 1997) and energy conversion between the energetic particles and the coronal plasmas. The breakup around the hot looptop may be another formation mode of solar eruptions in the chromosphere and corona. Observations indicate that some solar flares begin to erupt at somewhere above the plasma loops. It is possible that the cusp-like flares (Masuda et al. 1995) may be formed from the breakup of hot looptops by the MGP mechanism.

4. Conclusions and Discussions

The above analysis indicates that the MGP mechanism is a possible model for explaining the formation of hot plasma upflows, such as hot type II spicules observed by De Pontieu et al. (2009, 2011) and the hot plasma ejections along the ultrafine magnetic loop channels observed by Ji et al. (2012). It may provide another candidate to answer the coronal heating problem. With this mechanism, we obtain the following conclusions.

1. MGP mechanism can pick up the energetic charged particles from the underlying atmosphere and move them upward, forming hot plasma upflows, which pile up and accumulate in the upper

chromosphere and corona and finally cause the solar corona to become very hot. Energetic particles come from the underlying atmosphere, which is just the part of the high-energy tail in the thermal distribution function of the plasmas. A preliminary estimation indicates that this mechanism can cause the plasma temperature to reach about 10^4 K in the chromosphere, 10^5 K in the solar transition region, and 10^6 K in the corona. The energy flow is estimated to be about 8×10^6 erg cm^{-2}s^{-1} near the photosphere, 6×10^6 erg cm^{-2}s^{-1} in the chromosphere, 5×10^6 erg cm^{-2}s^{-1} in the transition region, and 7×10^5 erg cm^{-2}s^{-1} in the corona. Considering the inhomogeneous distribution of the magnetic field in the solar atmosphere, the above estimations are compatible with those in previous works (Withbroe & Noyes 1977; Aschwanden et al. 2007).

Additionally, the above estimations overlooked many important effects, such as energy release by magnetic reconnection, various wave damping, energy loss by radiation, and downflows from the plasma cooling, etc. Magnetic reconnection takes place in some small-scale regions with sheared magnetic configurations and wave damping and resonance absorptions occur in twisting magnetic configurations. Both are triggered by the underlying photospheric convective motions. Their releasing energy increases our above estimations around their action regions. At the same time, the energy loss caused by the downward flows or radiation of ion-neutral collisions in the partially ionized plasmas reduces the above estimations to some extent in the lower region near the photosphere and chromosphere. Different from these extremely dynamic processes, MGP is a steady, continuous, and ubiquitous process occurring in solar active regions, quiet regions, and in coronal holes. However, as we lack enough knowledge about the magnetic field distributions from the photosphere to the corona under present observations, it is very difficult to make an exact assessment of the changes of the above highly dynamic processes to our parameter estimations made by the MGP mechanism.

2. As for the three key questions we mentioned in Section 1, the MGP mechanism may present answers as follows. The energy heating the solar chromosphere and corona comes from the solar interior; the energetic charged particles are the energy carriers that are transported in the open magnetic flux tubes or closed magnetic flux loops by the MGP mechanism; the energetic particles deposit and spread their energy through thermal collisions, plasma instability triggered by temperature anisotropy, or the magnetic confinement damage. The great number of open magnetic flux tubes and closed magnetic flux loops with various space scales and considerable magnetic gradients in the solar atmosphere make the solar corona become hot. Additionally, as the upflow of the energetic charged particles takes away a fraction of energy from the underlying atmosphere, this will make the underlying atmosphere a bit cooler. This fact can explain why the regions with strong magnetic fields (such as in sunspot regions) near the solar surface have relatively low temperatures than the adjacent regions.

3. In the MGP mechanism, the solar open magnetic flux tubes and closed magnetic flux loops play a key role, acting as pumpers to extract the energetic particles from the underlying thermal plasma, and transport them to and deposit them in the upper atmosphere (chromosphere and corona). This process creates a hot upflow with a velocity of about 40 km s^{-1} in the chromosphere and about 130 km s^{-1} in the corona. The estimated velocities of upflows are very close to the observations of type II spicules, which provides a natural explanation of the formation of type II hot spicules and the upward injections of hot plasma stretching from the photosphere to the base of the solar corona.

However, the above estimations from the MGP mechanism are very rough. Because the most important parameter in the above estimations is the magnetic gradient (∇B), which dominates the final results and will change continuously from the solar surface to the upper corona and from the quiet region to the active region. So far, however, we have no reliable measurement of the magnetic fields from the chromosphere to the corona. Gelfreikh (1997) developed a method for estimating the coronal magnetic field on the basis of polarization inversion due to ordinary and extraordinary mode coupling in the coronal region of quasi-transverse propagation of radio observations. It can simultaneously provide the strength and gradient of the coronal magnetic field from imaging observations with high accuracy and high spa-

tial resolution. When the new radio telescope arrays such as the Chinese Spectral Radioheliograph (Yan et al. 2009) and the American Frequency Agile Solar Radiotelescope (Bastian et al. 2003) with broadband frequency and high spectral-spatial resolutions, come into service, it will be possible to obtain the three-dimensional magnetic maps of the solar chromosphere and corona. Subsequently, a reasonable estimation of the temperatures, density, and the velocity of upflows can be obtained by the method proposed in this work.

The MGP mechanism, in its essence, implies that the inhomogeneous magnetic fields coupling with plasmas will result in an inhomogeneous distribution of plasma temperature. As magnetic fields with a considerable gradient are ubiquitous in other stars, it is possible to use the MGP mechanism to explain many phenomena occurring in the stellar atmosphere such as the hot stellar corona and some ejections. In astrophysical conditions, high speed jets are observed frequently, these are called astrophysical jets (Meier et al. 1997). In fact, the magnetic fields in the source regions related to these jets are most similar to open flux tubes with considerable magnetic gradients. Such a magnetic configuration can naturally produce the hot upflows with high speed. For example, the plasma temperature may exceed 10^7 degrees in the solar flaring region and the adjacent atmosphere of black holes.

However, so far, coronal heating is still not resolved. The next step in the work of the MGP model is to deduce the magnetic gradient profile from the solar surface to the corona based on global MHD models and new spectral imaging observations, then derive the temperature profile and make a comprehensive comparison of this profile to other observational results, such as the STEREO EUVI data (Vazquez et al. 2010).

The author thanks the referee for helpful and valuable comments on this paper. Prof. J.Q. Dong and L.W. Yan provided important suggestions. Dr. Y. Zhang was a great help in improving the manuscript's language. This work is supported by NSFC grants 11273030, 11373039, 11221063, 11433006, and MOST grant 2011CB811401.

REFERENCES

Altschuler, M.D., Lilliequist, C.G., & Nakagawa, Y. 1968, SoPh, 5, 366

Aschwanden, M.J., Winebarger, A., Tsiklauri, D., & Peter, H. 2007, ApJ, 659, 1673

Aschwanden, M.J., & Nightingale, R.W. 2005, ApJ, 633, 499

Bastian, T.S. 2003, AdSpR, 32, 2705

Cargill, P.J., & Klimchuk, J.A. 2004, ApJ, 605, 911

Centeno, R., Socas-Navarro, H., Lites, B., et al. 2007, ApJ, 666, 137

Chen, L., & Wu, D.J. 2012, ApJ, 754, 123

Davila, J. 1987, ApJ, 317, 514

De Pontieu, B., McIntosh, S.W., Carlsson, M., et al. 2011, Sci, 331, 55

De Pontieu, B., McIntosh, S.W., Hansteen, V.M., Schrijver, C. 2009, ApJL, 701, L1

De Pontieu, B., McIntosh, S.W., Carlsson, M., et al. 2007, Sci, 318, 574

Dong, J.Q., Chen, L., Zonca, F. 1999, NucFu, 39, 1041

Edlen, B. 1943, ZA, 22, 30

Filippov, B., Koutchmy, S., & Vilinga, J. 2007, A&A, 464, 1119

Filippov, B., Golub L., & Koutchmy, S. 2009, SoPh, 254, 259

Fisk, L.A., & Schwadron, N.A. 2001, ApJ, 560, 425

Gelfreikh, G.B., Pilyeva N.A., & Ryabov, B.I. 1997, SoPh, 170, 253

Golub, L., Krieger, A.S., Harvey, J.W., Vaiana, G.S. 1977, SoPh, 53, 111

Greenwald, M. 2002, PPCF, 44, 27

Greenwald, M., Terry, J.L., Wolfe, S.M., & et al. 1988, NucFu, 28, 2199

Haas, F.A., & Thomas, C.L. 1973, PhFl, 16, 152

Habbal, S.R., & Withbroe, G.L. 1981, SoPh, 69, 77

Heyvaerts, J., & Priest, E.R. 1983, A&A, 117, 220

Hagyard, M.J., Teuker, D., Tandberg-Hanssen, E., et al. 1983, SoPh, 84, 13

Hahn, M., & Savin, D.W. 2013, ApJ, 763, 106

Hollweg, J.V. 2006, JGRA, 111, A12106

Inverarity, G.W., & Priest, E.R. 1997, in ASP Conf. Ser. 111, Magnetic Reconnection in the Solar Atmosphere, ed. R.D. Bentley & J.T. Mariska (San Francisco, CA:ASP), 296

Jess, D.B., Mathioudakis, M., Erdelyi, R., et al. 2009, Sci, 323, 1582

Ji, H.S., Cao, W.D., & Goode, P.R. 2012, ApJL, 750, L25

Klimchuk, J. 2006, SoPh, 234, 41

Kerr, R.A. 2012, Sci, 336, 1099

Landolfi, M. 1987, SoPh, 109, 287

Lemen, J. R., Title, A. M., Akin, D.J., et al. 2012, SoPh, 275, 17

Lin, H.S. 1995, ApJ, 446, L421

Lin, H.S., & Rimmele, T. 1999, ApJL, 514, L448

Litwin, C.; & Rosner, R. 1993, ApJ, 421, 375

Liu, Y., Wang, J.X., Yan, Y.H., & Ai, G.X. 1996, SoPh, 169, 79

López Fuentes, M. C., Klimchuk, J. A., Démoulin, P. 2006, ApJ, 639, 459

Masuda, S., Kosugi, T., Hara, H., Sakao, T., Shibata, K., & Tsuneta, S. 1995, PASJ, 47, 677

Mathew, S.K., & Ambastha, A. 2000, SoPh, 197, 75

Meier, D.L., Edgington, S., Godon, P., Payne, D.G., Lind, K.R. 1997, Natur, 388, 350

Narain, U., & Ulmschneider, P. 1996, SSRv, 75, 453

Parker, E.N. 1988, ApJ, 330, 474

Parashar, T.N., Velli, M., & Goldstein, B.E. 2013, in AIP Conf. Proc. 1539, Solar Wind 13 ed. Gary, P. Z., Joe, B., Roberto, B., et al.(Melville, NY: AIP), 54

Priest, E.R., Heyvaerts, J.F., & Title A.M. 2002, ApJ, 576, 533

Pneuman, G.W. 1983, ApJ, 265, 468

Pneuman, G.W. 1984, SoPh, 94, 387

Rappazzo, A.F., Velli, M., Einaudi, G., & Dahlburg, R.B. 2008, ApJ, 677, 1348

Reid, H.A.S., & Ratcliffe, H. 2014, RAA, 14, 805

Schluter, A., 1957, IAUS, 4, 356

Sturrock, P.A. 1999, ApJ, 521, 451

Takakura, T., & Scalise, E. 1970, SoPh, 11, 434

Van Ballegooijen, A.A., Asgari-Targhi, M., Cranmer, S.R., & DeLuca, E.E. 2011, ApJ, 736, 3

Vasquez, A.M., Frazin, R.A., & Manchester IV, W.B. 2010, ApJ, 715, 1352

Verth, G., Goossens, M., & He, J.S. 2011, ApJL, 733, L15

Vernazza, J.E., Avrett, E.H., & Loeser, R. 1981, ApJS, 45, 635

Walsh, R.W., & Ireland, J. 2003, A&ARv, 12, 1

Wedemeter-Böhm, S., Scullion, E., Steiner, O., et al. 2012, Natur, 486, 505

Withbroe, G.L., & Noyes, R.W. 1977, ARA&A, 15, 363

Wu, D.J., & Fang, C. 2003, ApJ, 596, 656

Yan, Y.H., Zhang, J., & Wang, W., et al. 2009, EM&P, 104, 97

Zhang, J., & Liu, Y. 2011, ApJL, 741, L7

Zwaan, C. 1978, SoPh, 60, 213

This 2-column preprint was prepared with the AAS LaTeX macros v5.2.